Metabolomic Characterization of Human Rectal Adenocarcinoma with Intact Tissue Magnetic Resonance Spectroscopy

Published in final edited form as:
Dis Colon Rectum. 2009 March ; 52(3): 520–525. doi:10.1007/DCR.0b013e31819c9a2c.

Metabolomic Characterization of Human Rectal Adenocarcinoma With Intact Tissue Magnetic Resonance Spectroscopy

Kate W. Jordan, B.A.[1], **Johan Nordenstam, M.D.**[3], **Gregory Y. Lauwers, M.D.**[1], **David A. Rothenberger, M.D.**[3], **Karim Alavi, M.D.**[3], **Michael Garwood, Ph.D.**[4], and **Leo L. Cheng, Ph.D.**[1,2]

[1]Department of Pathology, Massachusetts General Hospital, Harvard Medical School, Boston, Massachusetts

[2]Department of Radiology, Massachusetts General Hospital, Harvard Medical School, Boston, Massachusetts

[3]Department of Surgery, University of Minnesota, Minneapolis, Minnesota

[4]Center for Magnetic Resonance Research, University of Minnesota, Minneapolis, Minnesota

Abstract

Purpose—This study was designed to test whether metabolic characterization of intact, unaltered human rectal adenocarcinoma specimens is possible using the high-resolution magic angle spinning proton (^{1}H) magnetic resonance spectroscopy technique.

Methods—The study included 23 specimens from five patients referred for ultrasonographic staging of suspected rectal cancer. Multiple biopsies of macroscopically malignant rectal tumors and benign rectal mucosa were obtained from each patient for a total of 14 malignant and 9 benign samples. Unaltered tissue samples were spectroscopically analyzed. Metabolic profiles were established from the spectroscopy data and correlated with histopathologic findings.

Results—Metabolomic profiles represented by principle components of metabolites measured from spectra differentiated between malignant and benign samples and correlated with the volume percent of cancer (P=0.0065 and P=0.02, respectively) and benign epithelium (P=0.0051 and P=0.0255, respectively), and with volume percent of stroma, and inflammation.

Conclusions—Magnetic resonance spectroscopy of rectal biopsies has the ability to metabolically characterize samples and differentiate between pathological features of interest. Future studies should determine its utility in *in vivo* applications for non-invasive pathologic evaluations of suspicious rectal lesions.

Keywords

Rectal cancer; Metabolomics; Diagnosis; Magnetic resonance spectroscopy

Rectal cancers account for approximately one-third of colorectal malignancies, and the estimated number of cases for 2008 is 40,740.[1] The expected overall five-year survival rate for patients with a diagnosis of rectal cancer is 65 percent in the United States, according to

Address of correspondence: Leo L. Cheng, Ph.D., Pathology Research, CNY-7, 149 13th Street, Charlestown, Massachusetts 02129. E-mail: E-mail: cheng@nmr.mgh.harvard.edu.

Read at the meeting of the International Society for Magnetic Resonance in Medicine, Toronto, Ontario, Canada, May 3 to 9, 2008.

the National Cancer Institute.[2] Despite known prognostic factors and new and improved diagnostic methods, the severity of cancer stage is frequently underestimated.[3] Accurate diagnosis, staging, and management of the disease are crucial for achieving optimal outcomes. Currently, although histopathologic evaluation of biopsy samples can achieve most of these goals, radiologic tests such as computed tomography (CT), ultrasonography (US), positron emission tomography (PET), and magnetic resonance imaging (MRI) are unable to differentiate malignant from benign tissue with sufficient accuracy to be clinically useful for noninvasive diagnosis. The preoperative staging of the tumor is usually done according to the TNM system by using MRI, endorectal US, CT, or a combination of these tests to assess the tumor itself, whether it has spread to locoregional lymph nodes, and whether distant metastases are present.[4, 5]

The diagnosis of rectal cancer is currently dependent on biopsies taken from the suspicious lesion during colonoscopic or sigmoidoscopic examinations. Although histopathology will remain the standard for the diagnosis of rectal cancer for years to come, it is desirable to develop new technologies that not only can detect suspicious sites on direct biopsy, but may even replace histopathology to achieve diagnosis and grading of rectal cancer tumors noninvasively *in vivo*. Feasible techniques currently being examined for their potential roles in cancer management are those that probe the underlying biochemistry accompanying malignant changes, such as magnetic resonance spectroscopy (MRS). High-resolution magic angle spinning (HRMAS) proton (^{1}H) MRS is one such technique developed for the metabolomic analysis of intact tissues.[6, 7] The HRMAS ^{1}HMRS technique allows acquisition of highly resolved spectra from unaltered tissue samples, while preserving tissue histopathologic architecture for histopathologic analysis. Since its development, several groups, including our own, have shown the ability of this technique to differentiate malignant from benign samples of various tissues and to accurately characterize the bioactivity and, therefore aggressiveness, of tumors.[8, 9] The aim of the present study was to test the efficacy of the HRMAS ^{1}HMRS technique in differentiating malignant rectal cancer from benign cells by measuring the metabolic profile of rectal tumor biopsy samples and comparing them with benign rectal mucosa samples from the same patients.

Patients and Methods

Patients

Patients referred for ultrasonographic staging of suspected rectal cancer at the University of Minnesota were asked to participate in the study. The first five patients who agreed to participate were included in the pilot cohort reported here. Written informed consent to obtain ultrasonography-guided multiple biopsies from the tumor and benign rectal mucosa was obtained. Approval from the Institutional Review Board of the University of Minnesota was obtained before study initiation.

Biopsy samples

Biopsies of untreated rectal lesions that appeared malignant on US examination and on macroscopic examination with rigid sigmoidoscopy were obtained from each patient. One to two biopsies from macroscopically benign rectal mucosa were also obtained from each patient by inserting biopsy forceps through the rigid sigmoidoscope. The biopsy samples were immediately stored in cryo vials, de-identified (blinded), labeled, and put on dry ice. The samples were stored at −70°C until shipped overnight, on dry ice, to the Massachusetts General Hospital for spectroscopy and quantitative histopathology analyses.

High-resolution magic angle spinning proton magnetic resonance spectroscopy

Spectral analysis was performed on an Avance spectrometer (Bruker, Billerica, MA) operating at 600 MHz (14.1 T). Tissue samples were placed in a 4-mm rotor with plastic inserts creating a spherical sample space of ~10 ml located at the center of the detection coil. Approximately 2.0 μl of D_2O was added into the rotor with the tissue sample for field locking. All spectroscopy measurements were carried out at 4°C for tissue preservation. A repetition time of five seconds with 32 transients was used to acquire each spectrum. Spectra were collected with spinning rates of 3600 Hz. A rotor-synchronized Carr–Purcell–Meiboom–Gill (CPMG) filter (10 ms) was included in the pulse sequence to reduce broad resonances associated with probe and rotor background or macromolecules.

Spectroscopic data were processed with commercial software (Nuts, Acorn NMR Livermore, CA). All free induction decays were subjected to 1-Hz apodization before Fourier transformation, baseline correction, and phase adjustments of both zero and first order. Resonance intensities reported here represent integrals of curve-fittings with Lorentzian-Gaussian line shapes. Each sample produced well-resolved spectra with more than 50 quantifiable metabolites or regions. The 25 most intense resonance peaks were normalized by the total spectral intensity of the metabolite region up-field from water resonance (0.5~4.5 ppm), and then selected for further statistical analyses. All spectra were processed manually and objectively, without knowledge of tissue pathologic information.

Histopathology

After spectroscopic measurements were made, the samples were formalin fixed, embedded in paraffin, cut into 5-μm sections, and stained with hematoxylin and eosin. Sets of serial sections cut 150 μm apart were obtained from each sample. Percentages of the major pathologic components (cancer, benign epithelium, stroma, and inflammation) were visually estimated by a pathologist, and percentage of volume was calculated using a BX41 Microscope Imaging System (Olympus, Melville, NY), in conjunction with the image analyzer MicroSuite (Soft Imaging System, Lakewood, CO), as previously described.[8]

Statistical Analysis

Principle component analysis (PCA) was used to test the hypothesis that different pathologic components have differing metabolite profiles. This method was used to identify spectral metabolite profiles that correlated with pathologic features of the tissue, such as percentages of volume consisting of malignant cells, benign epithelium, stromal cells, and inflammation. An illustration of the PCA process can be found in Figure 1. The metabolite matrix was simplified such that 25 spectral regions with intensity means above the median determined from means calculated for all regions were subjected to PCA with statistical software JMP® (SAS Institute, Cary, NC). Principle component analysis identifies combinations of metabolites whose standardized concentrations (the difference between the particular intensity of the concerned metabolite for a particular sample and the mean intensity normalized by the standard deviation, both calculated for the metabolite from the entire sample set) are indicative of changes in the matrix that likely result from pathologic differences present among the analyzed samples. The principle components (PCs) consist of individual loading factors for each spectral region that are unique to the principle component and that indicate the extent to which the metabolites within that region are associated with the process described by the principle component. Thus, principle components are independent of one another.

The first seven principle components (with eigenvalues >1.0) were subjected to paired Student's *t* tests to investigate the ability of each component to differentiate malignant from benign samples. Simple linear regression analysis was used to test for correlations, with principle component scores as explanatory variables and pathologic features (volume

percentage of malignant cells, benign epithelium, stromal cells, or inflammation) as response variables.

Results

In this pilot study, a total of 23 samples were collected from five patients and analyzed. The results of histopathologic examination are shown in Table 1. Macroscopically, 14 samples were judged malignant and 9 benign. Histologic examination showed that samples from four patients (cases 2–5) had been correctly categorized on the basis of macroscopy as being malignant tissue or benign mucosa; samples deriving from suspected cancerous tissue from one patient (case 1) did not contain malignant cells.

Comparison of malignant *vs*. benign tissue samples showed significant differences for the three principle components, as listed in Table 2, together with their eigenvalues, percentages of variances represented, and cumulative percentages of variances. In addition to this binary differentiating capacity, linear regression analysis showed several principle components had predictive value, summarized in Table 3. For instance, PC 2, accounted for 16.1 percent of the variance among the samples, correlated negatively with volume percentage of malignant tissue (P=0.0065, slope=−0.0966, *Pearson's Correlation coefficient* r=−0.550) and positively with volume percentage of normal epithelium (P=0.0051, slope=0.0367, and r=0.564)..

The major loading factors for the regions that most significantly correlated with variations described by the principle components are shown in Table 4. For instance, PC 2 reflected changes in several metabolites with known connections to oncologic developments, including choline and phosphocholine.[10] Metabolic activity, including choline metabolites in the spectral region from 3.20 to 3.24 ppm, which significantly contributed to the differentiation of the normal from cancerous profile established by PC 2, is shown for one pair of samples (tumor and benign from patient 3) in Figure 2.

As indicated by Table 4, the most significant loading factors of each principle component, i.e., those with larger "+" or "-" values, present the positive or negative contributions of the concerned metabolites represented by their corresponding standardized concentration. For example, if the linear regression fit for a principle component with cancer is negative (slope<0), a negative loading factor for the choline metabolites in the 3.20- to 3.24-ppm region suggests that elevation of these metabolites above the calculated mean from all samples, and the reduction of metabolites in the 3.63–3.65 ppm region from their mean, contributes to the malignant profile, as seen with PC 2 in Table 4.

Discussion

Metabolomics and the HRMAS ^{1}HMRS Technique

The HRMAS ^{1}HMRS technique is an advanced metabolomics methodology. Metabolomics is the science of examining the unique chemical fingerprint of a cell, tissue, or organ by measuring the global variation of metabolites present (the metabolome). The metabolome may represent dynamic and physiologic changes that take place at the cellular level and that manifest themselves as changes in metabolite concentrations before pathologic changes can be seen on a static histologic slide. In this way, metabolomics offers a means by which malignant potential may be quantified before the malignancy changes the cellular architecture. This hypothesis is the basis of what can be described as oncologic metabolomics. The HRMAS ^{1}HMRS technique was developed specifically for the analysis of intact, unaltered tissue samples. This deviates from classical NMR of aqueous solutions and other magnetic resonance techniques, which require that metabolites be extracted from the tissue of interest, destroying the tissue and precluding histopathologic analysis. The histopathology is crucial, however, as it allows

correlation of the specific metabolite profiles with the characteristics of interest (in this study, the presence or absence of malignant cells). The utility of the HRMAS ^{1}HMRS method is further increased by its ability to be automated and free from issues of inter-observer reproducibility.

Differentiation of Cancerous from Benign Samples

Currently, histopathologic examination can reliably differentiate benign from malignant tissues for clinical diagnosis and was the standard used in this pilot study. We used histopathologic validation to determine whether metabolite profiles for human rectal adenocarcinoma biopsy samples constructed with HRMAS ^{1}HMRS in the same manner as that created for various other tissues might have the potential to improve the current state of radiology for noninvasive *in vivo* rectal adenocarcinoma diagnosis. Each of the four pathologic features examined (malignant cells, benign epithelium, stromal cells, and inflammation) manifested different biochemical changes that could be significantly delineated by PCA. The principle components that correlated with volume percentages of tumor or benign mucosa were most noteworthy.

Interestingly different principle components that correlated with the same process could have metabolite regions that contributed to the process in the same manner but with differing magnitudes, or they could have metabolite regions that contributed in different ways. For example, increases in metabolites in the 3.41- to 3.47-ppm region were related to the malignant condition for both PC 2 and PC6). However, metabolites in the 3.66- to 3.68-ppm region significantly contributed to PCs 2 and 6, but in opposite ways (diminished in the malignant condition in PC2, but elevated in the malignant condition in PC6).

The sensitivity of the current profiles may be limited by the mixed pathological features in the analyzed samples. By incorporating a larger cohort of samples and additional features, the metabolite profiles might be further refined.

Implications and Limitations of the Current Study

Results from the current study are encouraging because they show that metabolic differences between samples containing different pathologic features can be significant enough to be measurable with HRMAS ^{1}HMRS. Such results have important implications for future research, particularly if additional features such as tumor grade or aggressiveness are found to manifest themselves in measurable metabolic differences. If further investigations are able to correlate clinical features with metabolic profiles, HRMAS ^{1}HMRS may be very useful for rectal adenocarcinoma, and may provide information that current *in vivo* radiologic means are unable to produce. One such factor of paramount clinical importance is tumor virulence, as defined by the likelihood of recurrence following curative surgery. Our examinations of human prostate cancer indicate metabolic profiles can subdivide similarly staged malignancies into groups according to aggressiveness of the primary tumor.[8] Although the current study, which was at the pilot level and therefore recruited only 5 subjects, is by no means an indication that such segregation of rectal tumors is possible with HRMAS ^{1}HMRS, it does suggest that future examinations toward this end are a valid undertaking. Because our subjects were recruited before treatment, the clinical outcomes are not known at this time and cannot be correlated with the metabolic information gathered.

Furthermore, given the potential of MRS-based metabolomic profiles in differentiating malignancy from benign tissues from the same patients, the ever increasing developments in the *in vivo* MR technologies may make it possible to use the present *ex vivo* techniques *in vivo*, and to inspire further technology developments targeted at investigations of *in vivo* noninvasive MRS in the detection and characterization of human rectal adenocarcinomas.

Conclusion

As an exploratory study designed to test of the efficacy of the HRMAS ^{1}HMRS method in metabolically characterizing human rectal adenocarcinomas, the current results are significant and encouraging. The results indicate that magnetic resonance may be useful in the *ex vivo* biochemically classification of tissue samples as malignant or benign. In addition to the possibility of future *in vivo* use, further studies may reveal whether HRMAS ^{1}HMRS, can accurately stage rectal tumors or indicate additional prognostic factors, such as a subset of more aggressive tumors that should be monitored postsurgery for recurrence.

Acknowledgments

Supported by grants from the National Institutes of Health (CA115746, CA095624), and the Massachusetts General Hospital A. A. Martinos Center for Biomedical Imaging.

REFERENCES

1. Jemal A, Siegel R, Ward E, et al. Cancer statistics, 2008. CA Cancer J Clin 2008;58:71–96. [PubMed: 18287387]
2. SEER. Stat Fact Sheets - Cancer of the Colon and Rectum. 2008 [Accessed December 1 2008]. Available at: http://seer.cancer.gov/statfacts/html/colorect.html
3. Tepper JE, O'Connell MJ, Niedzwiecki D, et al. Impact of number of nodes retrieved on outcome in patients with rectal cancer. J Clin Oncol 2001;19:157–163. [PubMed: 11134208]
4. Brown G, Richards CJ, Newcombe RG, et al. Rectal carcinoma: thin-section MR imaging for staging in 28 patients. Radiology 1999;211:215–222. [PubMed: 10189474]
5. Garcia-Aguilar J, Pollack J, Lee SH, et al. Accuracy of endorectal ultrasonography in preoperative staging of rectal tumors. Dis Colon Rectum 2002;45:10–15. [PubMed: 11786756]
6. Cheng LL, Lean CL, Bogdanova A, et al. Enhanced resolution of proton NMR spectra of malignant lymph nodes using magic-angle spinning. Magn Reson Med 1996;36:653–658. [PubMed: 8916014]
7. Cheng LL, Ma MJ, Becerra L, et al. Quantitative neuropathology by high resolution magic angle spinning proton magnetic resonance spectroscopy. Proc Natl Acad Sci U S A 1997;94:6408–6413. [PubMed: 9177231]
8. Cheng LL, Burns MA, Taylor JL, et al. Metabolic characterization of human prostate cancer with tissue magnetic resonance spectroscopy. Cancer Res 2005;65:3030–3034. [PubMed: 15833828]
9. Sitter B, Lundgren S, Bathen TF, et al. Comparison of HR MAS MR spectroscopic profiles of breast cancer tissue with clinical parameters. NMR Biomed 2006;19:30–40. [PubMed: 16229059]
10. Podo F. Tumour phospholipid metabolism. NMR Biomed 1999;12:413–439. [PubMed: 10654290]

	P1	*P2*	*P3*		*P24*	*P25*
S1	p1,1	p2,1	p3,1		p24,1	p25,1
S2	p1,2	p2,2	p3,2		p24,2	p25,2
S3	p1,3	p2,3	p3,3		p24,3	p25,3
S22	p1,22	p2,22	p3,22		p24,22	p25,22
S23	p1,23	p2,23	p3,23		p24,23	p25,23

PCA

	PC1	*PC2*	*PC3*		*PC22*	*PC23*
P1	c1,1	c2,1	c3,1		c22,1	c23,1
P2	c1,2	c2,2	c3.2		c22,2	c23,2
P3	c1,3	c2,3	c3,3		c22,3	c23,3
P24	c1,24	c2,24	c3,24		c22,24	c23,24
P25	c1,25	c2,25	c3,25		c22,25	c23,25

S#: Sample #; **P#:** Peak #; **$p\#^{P},\#^{S}$:** Standardized concentration for Peak $\#^{P}$ of Sample $\#^{S}$;
PC#: Principal component #; **$c\#^{PC},\#^{P}$:** Loading factor for $PC\#^{PC}$ of $Peak\#^{P}$.

Example for PC value calculation:

PC3 for Sample 2 = A-(c3,1*p1,2+c3,2*p2,2 +c3,3*p3,2+ … +c3,25*p25,2);
A=constant.

Figure 1.

Illustration of principal component analysis (PCA). This process starts with the top S-P matrix, where S and P represent samples and spectral peaks, respectively, and p#,# is the value of the standardized peak concentration. Standardized concentration refers to the difference between the particular intensity of the concerned metabolite for a particular sample and the mean intensity normalized by the standard deviation, with both mean and standard deviation values calculated for the metabolite from the entire sample set. From this S-P matrix, the PCA process generates a principal component (PC) coefficient matrix (bottom) to be used to form PCs of linear combinations of the standardized peak concentrations. All PCs are orthogonal to each

other, with PC1 representing the greatest and PC23, the least changes in the standardized peak concentrations.

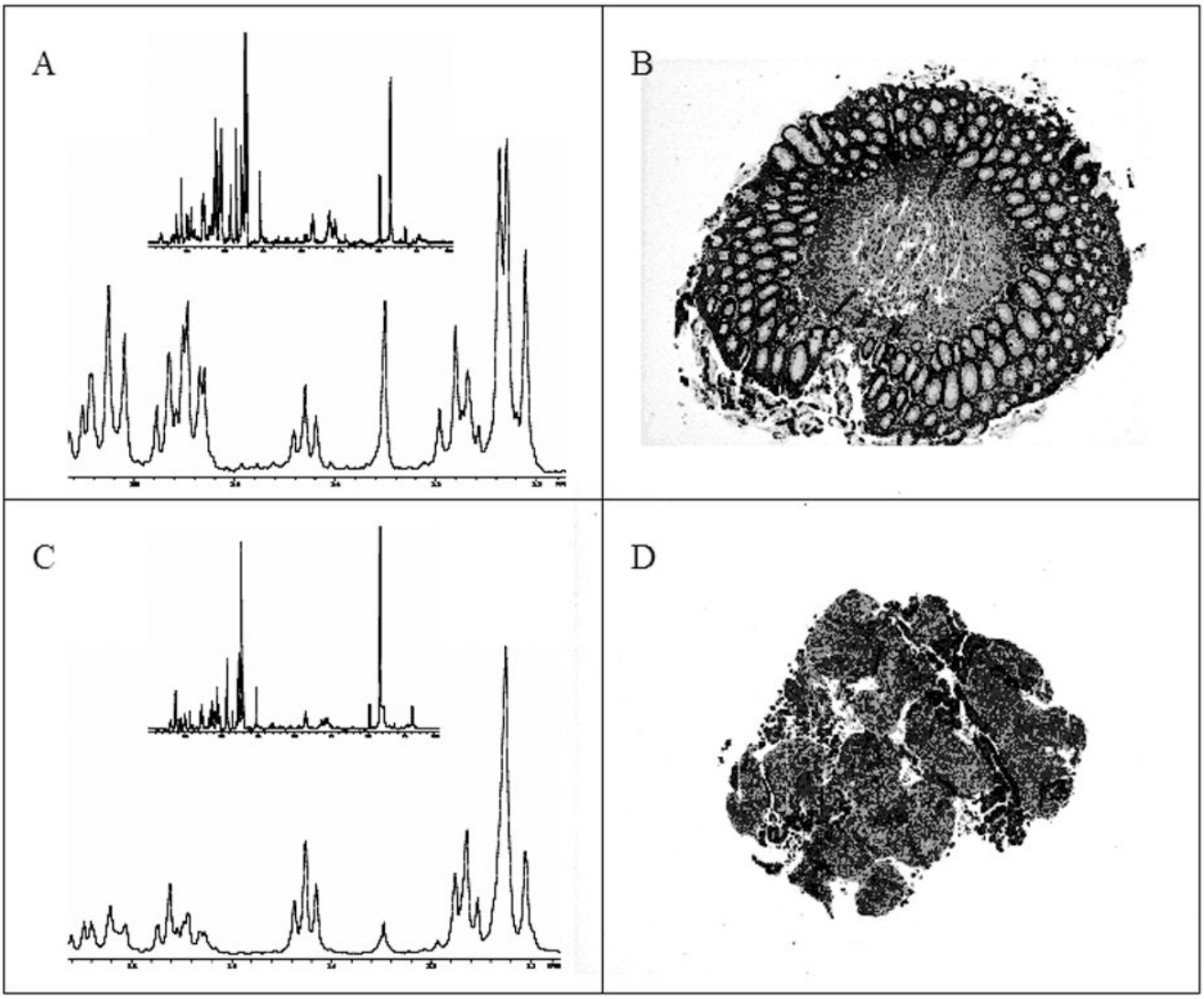

Figure 2.

A) HRMAS ^{1}HMRS spectrum of Patient 3, sample ii (benign mucosa); entire metabolite spectrum (top) and enlargement of the 3.2–3.7 ppm area, which significantly contributed to the variation in PC 2; B) Sample 3-i contained 0 percent malignant cells, 70 percent benign epithelium, 20 percent stromal tissue, and 10 percent inflammation; C) Spectrum from Patient 3, sample iv (tumor tissue), entire spectrum (top) and enlargement of the 3.2–3.7 ppm area; D). Sample 3 iv contained 20 percent malignant cells, 0 percent benign epithelium, 60 percent stromal tissue, and 20 percent inflammation.

Table 1

Complete pathology report for 23 biopsy samples from 5 patients

Pat. no.#	Sample	Macroscopic designation	Cancer %	Benign epithelia, %	Stroma %	Inflammation %	Final designation
1	i	Malignant	0	70	20	10	Benign
1	ii	Malignant	0	70	20	10	Benign
1	iii	Benign	0	70	10	20	Benign
1	iv	Benign	0	70	20	10	Benign
2	i	Benign	0	60	30	10	Benign
2	ii	Malignant	10	0	70	20	Malignant
2	iii	Malignant	20	0	70	10	Malignant
2	iv	Malignant	30	0	60	10	Malignant
3	i	Benign	0	60	30	10	Benign
3	ii	Benign	0	70	20	10	Benign
3	iii	Malignant	10	30	40	20	Malignant
3	iv	Malignant	20	0	60	20	Malignant
4	i	Malignant	25	0	60	15	Malignant
4	ii	Malignant	25	0	40	35	Malignant
4	iii	Malignant	10	0	10	80	Malignant
4	iv	Malignant	10	0	75	15	Malignant
4	v	Malignant	30	0	50	20	Malignant
4	vi	Benign	0	40	50	10	Benign
4	vii	Benign	0	60	30	10	Benign
5	i	Malignant	30	40	20	10	Malignant
5	ii	Malignant	5	70	15	10	Malignant
5	iii	Benign	0	60	30	10	Benign
5	iv	Benign	0	40	40	20	Benign

Table 2

Identification of malignancy according to Student's t-tests

PC	Eigen Value	%	Cum%	Cancer (mean, std err)	Benign Epithelia (mean, std err)	P value
2	4.015	16.1	48.2	−0.989, 0.465	1.286, 0.530	0.0041
4	2.744	11.0	74.3	−0.667, 0.415	0.867, 0.473	0.0238
6	1.376	5.5	87.2	0.546, 0.280	−0.710, 0.319	0.0075

Table 3

Results of linear regression analysis

Feature (% sample volume)	P value	Slope	Pearson 's Correlation coefficient (r)
PC 2			
Cancer	0.0065	−0.0966	−0.550
Benign epithelium	0.0051	0.0367	0.564
PC 4			
Benign epithelium	0.0333	0.0240	0.445
Stroma	0.0311	−0.0343	−0.451
PC 6			
Cancer	0.0200	0.0494	0.482
Benign epithelium	0.0255	−0.0177	−0.465
PC 7			
Inflammation	0.0026	−0.0418	−0.598

Table 4

Loading factors and regions corresponding to principle components

Loading factor	Region (ppm)
PC 2 (correlates negatively with cancer and positively with benign epithelium)	
0.36331	3.65–3.63
0.36085	3.58–3.51
0.35388	3.68–3.66
0.22815	1.15–1.14
−0.35014	4.21–4.16
−0.32501	3.29–3.25
−0.28986	3.47–3.41
−0.2086	3.24–3.20
PC 4 (correlates positively with benign epithelium and negatively with stroma)	
0.29915	1.15–1.14
0.25695	1.36–1.28
0.25598	2.16–2.05
0.24953	3.62–3.59
0.24475	4.09–4.06
0.24294	0.92–0.84
0.1987	2.04–1.96
0.16453	3.24–3.20
0.16375	3.92–3.88
−0.4325	1.02–0.93
−0.30164	3.87–3.83
−0.28619	4.04–3.96
−0.26181	1.49–1.47
PC 6 (correlates positively with cancer and negatively with benign epithelium)	
0.36361	3.47–3.41
0.32365	2.40–2.34
0.27615	3.68–3.66
0.24947	2.48–2.41
0.24394	4.15–4.11
−0.45242	4.09–4.06
−0.28916	3.95–3.93
PC 7 (correlates positively with inflammation)	
0.21691	3.29–3.25
0.20066	3.24–3.20
0.18972	3.80–3.75
0.18171	2.48–2.41
0.13947	3.65–3.63
0.13223	0.92–0.84
0.11239	4.04–3.96
−0.7542	4.15–4.11

PC = principle component; ppm = parts per million.